Journal of Groundwater Science and Engineering
ISSN 2305-7068
Indexed by ESCI CABI CSA
Scopus GeoRef AJ CNKI

Estimating aquifer transmissivity using Dar-Zarrouk parameters to delineate groundwater potential zones in Alluri Seetharama Raju District, Andhra Pradesh, India

Bakuru Anandagajapathi Raju, Palavai Venkateswara Rao, Mangalampalli Subrahmanyam

Citation:
Raju BA, Rao PV, Subrahmanyam M. 2023. Estimating aquifer transmissivity using Dar-Zarrouk parameters to delineate groundwater potential zones in Alluri Seetharama Raju District, Andhra Pradesh, India. Journal of Groundwater Science and Engineering, 11(2): 116-132.

View online: https://doi.org/10.26599/JGSE.2023.9280011

Journal of Groundwater Science and Engineering 11(2023) 116–132

Journal homepage: http://gwse.iheg.org.cn

Research Paper

Estimating aquifer transmissivity using Dar-Zarrouk parameters to delineate groundwater potential zones in Alluri Seetharama Raju District, Andhra Pradesh, India

Bakuru Anandagajapathi Raju[1*], Palavai Venkateswara Rao[1], Mangalampalli Subrahmanyam[1]

[1] *Department of Geophysics, Colleges of Science & Technology, Andhra University, Visakhapatnam* 530003, *Andhra Pradesh, India*.

Abstract: This study aimed to explore groundwater potential zones in the EGMB of Alluri Seetharama Raju district, Andhra Pradesh, India, for drinking and agriculture purposes. To achieve this goal, 72 Vertical Electrical Soundings (VES) were conducted using the Schlumberger electrode configuration. The resistivity sounding data were analyzed to determine the aquifer thickness, basement depth, Dar-Zarrouk parameters, and aquifer transmissivity. Spatial distribution maps were generated for these parameters to understand the subsurface formation. The analysis revealed a linear groundwater potential zone (8.46 km^2) in the eastern part of the study area, extending in the NNE-SSW direction for 9.6 km. Six VES locations (P24, P27, P29, P30, P33, and P38) in this zone exhibit good potential (>30 m aquifer thickness), while the three VES locations (OP19, P5, and P46) in the central region are recommended for drilling bore wells. Additionally, moderate aquifer thickness (20–30 m) are identified in other VES locations (OP14, OP20, P4, P10, P12, P13, P15, P17, P18, P31, P46, and P50) along streams in the western and central part of the area, which can yield reasonable quantities of water. This information is useful for groundwater exploration and watershed management to meet the demands of tribal population in the study area.

Keywords: Vertical electrical sounding; Longitudinal conductance; Transverse resistance; Coefficient of anisotropy; Potential groundwater locations

Received: 20 Oct 2022/ Accepted: 30 Mar 2023/ Published: 15 Jun 2023

Introduction

Groundwater is a precious renewable natural resource on Earth, constituting only 0.61% of the total global water budget (Anandagajapathi et al. 2020; Seker and Efe, 2023; Danso and Ma, 2023). In recent years, groundwater exploitation has increased to meet the demand due to deterioration in quality of surface water resources. The occurrence, distribution, and movement of groundwater vary in time and space, and depends greatly on the types of rock formation as well as the degree of weathering and fracturing of the source rocks (Dor et al. 2011). A detailed study of the geology, geomorphology and hydrogeological aspects of any terrain is essential for effective groundwater extraction. In the case of metamorphic/ crystalline rocks, primary porosity and permeability are usually low, and groundwater extraction mainly depends on secondary porosity developed through weathering or fracturing in rocks (Maja et al. 2020). Geophysical methods, such as resistivity surveys, have been widely adopted to solve various hydrogeological problems in hard rock terrains (Ammar and Kruse, 2016; Kang et al. 2018; Deng et al. 2020; Rustadi et al. 2022). Surface geophysical measurements, along with remote sensing, can determine several parameters characterising water-bearing formations (Venkateswara et al. 2021). The resistivity survey is particularly popular low-cost (Sathiyamoorthy and Ganesan, 2018),

*Corresponding author: Bakuru Anandagajapathi Raju, *E-mail address*: anand.bakuru@gmail.com

DOI: 10.26599/JGSE.2023.9280011

Raju BA, Rao PV, Subrahmanyam M. 2023. Estimating aquifer transmissivity using Dar-Zarrouk parameters to delineate groundwater potential zones in Alluri Seetharama Raju District, Andhra Pradesh, India. Journal of Groundwater Science and Engineering, 11(2): 116-132.

providing good contrast in resistivity measurements of water-saturated and non-saturated rock formations (Loke et al. 2013, Subrahmanyam and Venkateswara, 2017b; Venkateswara et al. 2019b). The Vertical Electrical Sounding (VES) technique of the geophysical method has been effectively used by many researchers in diverse fields, including groundwater investigations (Hamzah et al. 2007; Gupta et al. 2012). The transformation of VES data of Schlumberger configuration to Radial dipole configuration can yield better results in cases of hidden (thin) layers (Subrahmanyam and Venkateswara, 2017a).

The Dar-Zarrouk (D-Z) parameters were first introduced by Maillet (1947) to address the issue of non-uniqueness in the interpretation of resistivity sounding curves in geoelectrical methods. These parameters are widely used to estimate aquifer parameters such as hydraulic conductivity and transmissivity (Ankidawa et al. 2019; Siva and Marykutty, 2019; Venkateswara et al. 2022) in porous media (e.g. alluvium formation) and fracture media (e.g. metamorphic and igneous) to identify groundwater potential zones. In recent studies, Nugraha et al. (2023) used D-Z parameters to estimate groundwater potential zones in fracture media. The longitudinal unit conductance (S) of the D-Z parameter is a measure of the impermeability of a rock layer and provides information on the highly resistive fresh basement topography as the depth to the basement (Ayolabi et al. 2010). According to Oteri (1981), a marked increase in S value may correspond to an average increase in the clay content, leading to a decrease in the transmissivity (T_r) of aquifer. Atakpo (2013) and Awni (2013) used this parameter to show the aquifer' s protective capacity. The transverse resistance (T) of the the D-Z parameter is used to study the variations in the thickness of high-resistivity materials (Zohdy, 1989). To improve the accuracy of geological mapping using an electrical resistivity surveys, the study of electrical resistivity anisotropy (λ) in rocks has become crucial (Olasehinde and Bayewu, 2011). The anisotropy of rocks can be caused by their fracturing or metamorphism, as well as the presence of disseminated ore grains. Lower values of λ are associated with high aquifer potential zones, according to recent studies by Venkateswara et al. (2022), Suneetha et al. (2021), and Shailaja et al. (2019).

The study area is situated in a hilly terrain, which is part of the Eastern Ghats Mobile Belt (EGMB), where people are still suffering from groundwater scarcity. Due to the challenging nature of water exploration in this area, it is crucial to conduct a comprehensive analysis of multi-parameters, including geophysical and associated hydrogeological parameters, to accuratedly locate groundwater potential zones. In this study, the geometry of the subsurface lithological units was investigated using D-Z parametric analysis, which is an effective tool for identifying potential groundwater zones. The D-Z values were then used to derive hydrogeological parameters, such as hydraulic conductivity and aquifer transmissivity. These parameters provide valuable information on the potential aquifer zones in the study area, helping to imporove groundwater exploration efforts.

1 Study area

The study area is located within the boundaries of Paderu revenue Mandal, which is the headquarters of the Alluri Seetha Rama Raju district of Andhra Pradesh, India (Fig. 1). It extends from 18.059 3° E to 18.760 5° E and 82.525 5° N to 82.760 5° N, which is part of the Matchkund river catchment.

The study area is situated at the top of the hilly tracts of the Eastern Ghat Mobile Belt (EGMB) and is designated as an integrated tribal development agency (ITDA) area by the Indian government due to its large population of scheduled tribes. The Matchkund river originates from G-Madugula hills at an altitude of 1 540 m AMSL and flows north through several revenue mandals of G-Madugula, Paderu, Hukumpeta, Pedabayalu, and Munchinigiputtu, before reaching the river Sabari in Odissa state. As shown in (Fig. 1 and Table 1), the distinctive lithological units of the Eastern Ghat Supergroup, including Khondalite, Charnockite, and Migmatites of Archaean age, are prominently exposed in the study area (GSI, 2001; Anandagajapathi et al. 2020). The geology map geological map used in this study was obtained from the Geological Survey of India.

The average annual rainfall in this study area is about 1 274 mm/a and groundwater occurs in shallow to unconfined conditions in the study area (CGWB, 2019). However, irregular topography cuases most precipitation to immediately convert into surface runoff in many areas of the region.

Geomorphological features as landform and topography are essential in watershed management and groundwater exploration (Fashae et al. 2014). The physical features of the earth's surface greatly influence the infiltration, runoff, and occurrence of groundwater. In this study, a geomorphological mapwas generated by digitizing was generated by digitizing different geomorphic units from the colour cloud-free Landsat-8 satellite data composite on 16th March 2022 using the visual image

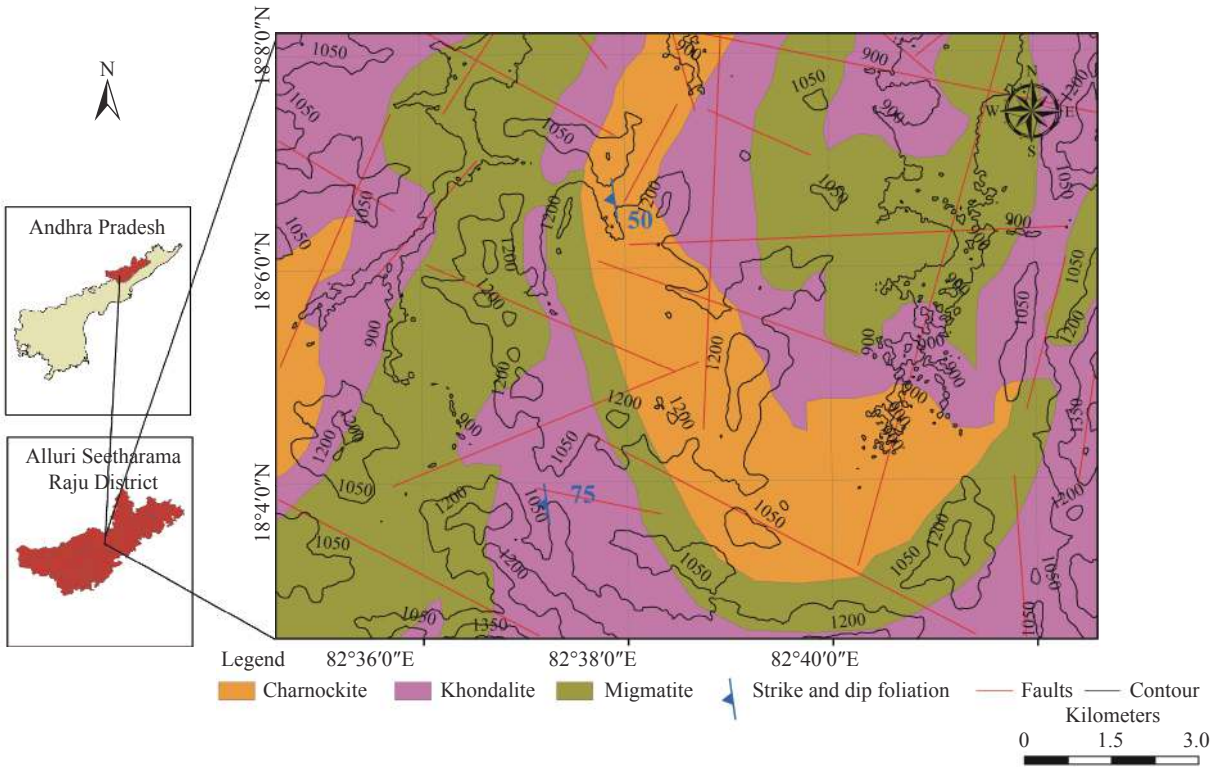

Fig. 1 Geology map of the study area

Table 1 Stratigraphic succession of geological formations in the study area

Geological formation	Characteristics
Migmatites	Hard, Foliated rocks
Charnockites (Basic, Acid, and intermediate)	Hard, Massive rocks
Khondalites	Hard, Foliated rocks

interpretation technique (color/tone/texture/pattern/association/size/shape) in ArcGIS. The study area consists of moderately dissected hills and valleys, a pediment-pediplain complex, and a river (Fig. 2). Two narrow streams flow through the study area in a south-to-north direction and join the Matchkund River, which flows north of the study area. The pediment-pediplain complex area surrounded by streams on the eastern side is about 25 km^2. Field observations indicate that the river's width increased from south to north, while a small portion of discontinued pediment-pediplain patches was identified on the western side of the study area.

2 Data and methodology

2.1 Lineaments

Lineaments, such as faults and joints, play a crucial role in storing and facilitating the movement of groundwater. As potential flow conduits, they are essential for groundwater study, particularly in hard rock areas. To create the lineament map, a reference was made to Bhuvan's thematic layer, and the map was generated in ArcGIS using Web Map Service (WMS). The final map was saved in vector format as the lengths of all lineaments can be calculated from vector files (Fig. 2). In the study area, all identified lineaments were of the structural category (faults/joints). These lineaments varied in length from 0.45 km to 9.6 km and had different orientations, including N-S, NE-SW, E-W, and SE-NW. A total of 22 lineaments were identified, of which 16 were minor (2–10 km), and 6 were micro (less than 2 km) lineaments (Table 2) (Sitharam et al. 2007; Venkateswara et al. 2021).

In the study area, there is a prominent lineament that runs for 9.6 km in the NNE-SSW direction on the eastern side, where the stream also flows. Additionally, several minor lineaments of varying lengths are scattered throughout the area (Fig. 2). The pediment-pediplain complex zones and lineaments play a crucial role in groundwater accumulation.

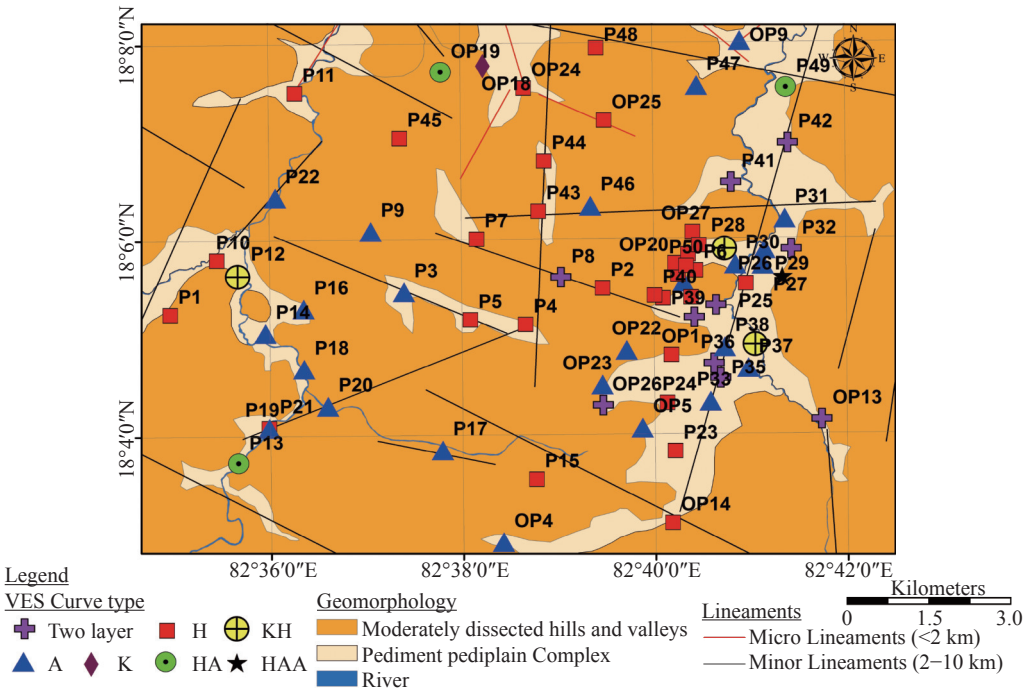

Fig. 2 Geomorphology and lineaments map of the study area with VES locations

Table 2 Classification of lineaments (Sitharam et al. 2006; Venkateswara et al. 2021)

No.	Type of the lineament	Length of the lineament	No. Lineaments identified in the area
1	Medium	10–100 km	-
2	Minor	2–10 km	16
3	Micro	<2 km	06

2.2 Geoelectrical surveys

A total of 72 Vertical Electrical Soundings (VES) were conducted in the study area using Schlumberger configuration, with a maximum half current electrode spacing (AB/2) of 130 m (Fig. 2 and Fig. 3). Most of the soundings were carried out by aligning the electrode system in the direction of the lineaments. All the soundings were conducted using a DDR3 resistivity meter of IGIS-Hyderabad. The apparent resistivity was the measured parameter for the surveys.

The comprehensive processing of VES data reveals that the study area consists of 2 to 5 subsurface lithological layers and exhibits apparent resistivity curves of two-layer ascending type, H, A, K, of three-layer, KH, and HA of four-layer and HAA of five-layer types (Fig. 2 and Fig. 3).

Based on Fig. 2, it can be inferred that in the eastern foothills where hard rock is located immediately beneath a thin soil layer, both two-layer ascending type and HAA curves are observed. In the eastern and western valleys and streams, where thick sediments cover the hard basement, A and KH-type curves are observed. In the central part of the area, where pediment-pediplain complex zones present, H and HA-type curves were found. The K-type curve was observed near the foothill in the northern part of the study area.

The collected VES data was initially interpreted manually using the partial curve matching technique of Zohdy (1965), and Orellana and Mooney (1966). The resulting parameters were used as initial guesses for the software IPI2Win (Bobachev, 2003), which accurately delineates different subsurface layers from the same VES curves, compared to software such as IRESAN and RESIST (Venkateswara et al. 2019a).

The apparent resistivity data from the VES were inputted into IPI2Win, where the software automatically suggests the best-fitting two-layered model for the initial interpretation. The model can be edited by changing the number of layers (from 2 up to 30), splitting or joining them and altering their properties on the screen. The layer properties can be edited in the table cells of the model window, and the theoretical curve is redrawn for the updated model parameters. The software iteratively updates the two-layer model into a multilayer problem until the synthetic curve calculated

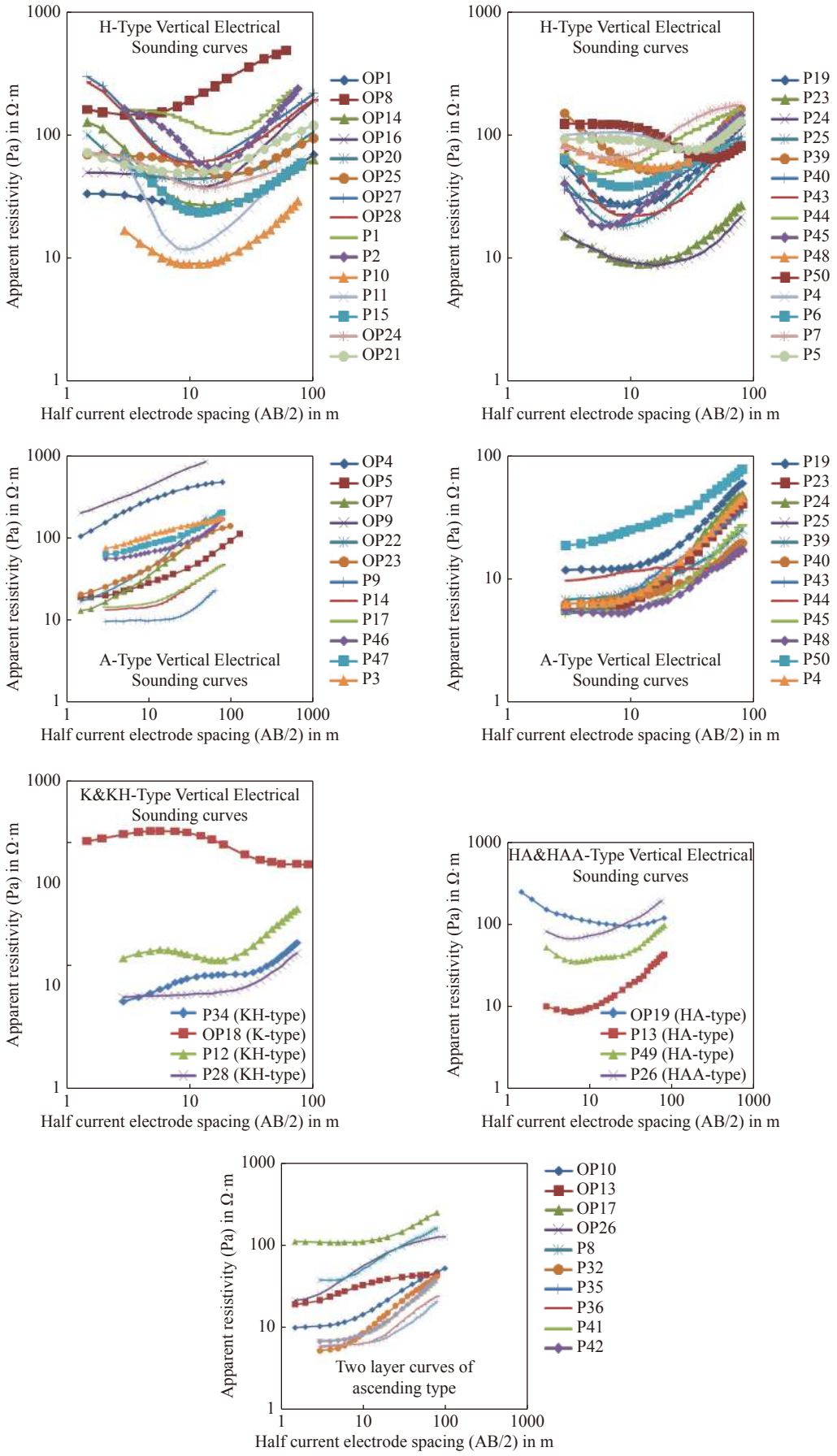

Fig. 3 Vertical electrical resistivity sounding curves obtained from the study area

with the program fits the field curve precisely, ensuring the RMS error is minimized. The obtained RMS error for the sounding data ranges from 0.35% to 4.34% (Table 3), with the minimum acceptable RMS error for the software being < 5%. The resulting primary geoelectrical parameters of the subsurface layers were used to determine the depth to the basement and aquifer thickness by measuring the total thickness of the overlying layers. Thereby, the spatial distribution maps of these two parameters were generated (Fig. 4a and Fig. 4b).

2.3 Other geo-electrical parameters

A geo-electric layer can be described by two primary parameters: Resistivity (ρ_i) and thickness (h_i) where the subscript 'i' denotes the position of the layer in the section. The secondary geo-electric parameters, such as total longitudinal conductance (S), total transverse resistance (T), longitudinal resistivity (ρ_l), transverse resistivity (ρ_t), and coefficient of anisotropy (λ), are derived from the primary parameters (Zohdy et al. 1974).

2.3.1 Total longitudinal conductance

Total longitudinal conductance (S) is the ability of current flow parallel to the geo-electrical layers, which represents the resistance parallel to the face of the prism Zohdy et al. (1974). S can be calculated using the following equation:

$$S = \sum_{i=1}^{n} \frac{h_i}{\rho_i} \quad (1)$$

Where: h_i and ρ_i represent the thickness and resistivity of the i^{th} layer, respectively. The variation in S from one location to another can be used to qualitatively document the changes in the total thickness of low-resistivity material (Zohdy, 1989). High S values are indicative of low aquifer transmissivities (Awni, 2013). According to the classification system proposed by Oladapo and Akintorinwa (2007), the S values can be used to grade the aquifer protective capacity from poor to excellent (Table 4).

Table 3 Rating of the protective capacity of aquifers (After Oladapo and Akintorinwa, 2007)

Total longitudinal conductance (Siemens)	Protective capacity rating
>10	Excellent
5–10	Very good
0.7–4.9	Good
0.2–0.69	Moderate
0.1–0.19	Weak
<0.1	Poor

2.3.2 Total transverse resistance

The total transverse resistance (T) is the resistance that is offered to the current flowing perpendicular to geo-electrical layers (Sathiyamoorthy and Ganesan, 2018). It can be calculated as

$$T = \sum_{i=1}^{n} h_{ii} \quad (2)$$

Where: h_i refers to the thickness, and the ρ_i denotes the resistivity of the i^{th} layer.

The higher values of transverse resistance (T) are used to study the variations in the thickness of high resistivity material, while lower values of T provide information about the weathering nature of the rocks (Venkateswara et al. 2022; Sri and Singhal, 1981). The parameters ρl and ρt are used to calculate the coefficient of anisotropy (λ). When ρ_l & ρ_t are equal, the sub-surface layers are

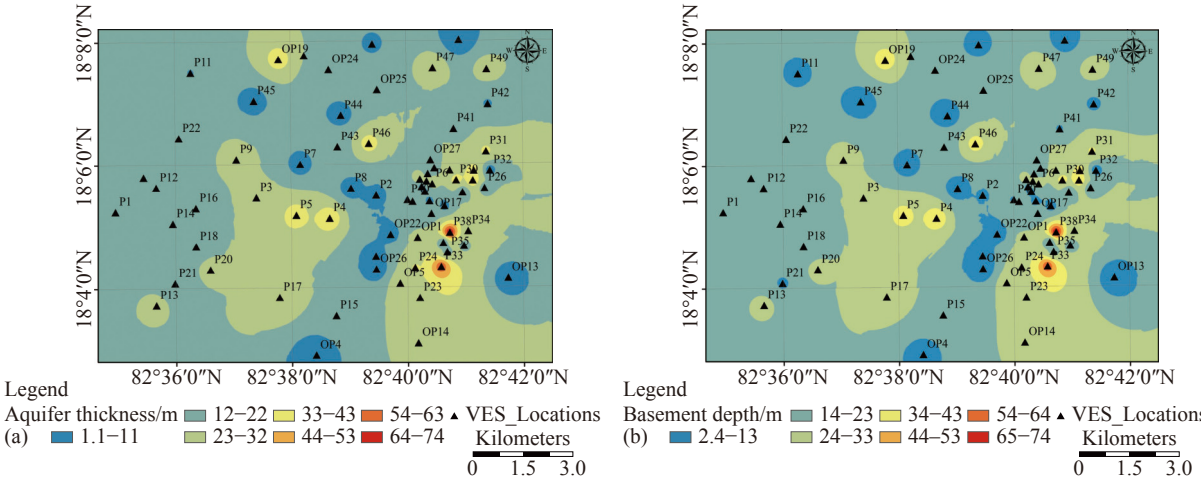

Fig. 4 Spatial distribution maps of (a) Aquifer thickness, and (b) Basement depth in the study area

Table 4 Interpreted layer parameters from VES data in the study area

VES code	Latitude degrees	Longitude degrees	True resistivity					Thickness				Total thickness /m	RMS error /%
			ρ 1 /Ω·m	ρ 2 /Ω·m	ρ 3 /Ω·m	ρ 4 /Ω·m	ρ 5 /Ω·m	h 1 /m	h 2 /m	h 3 /m	h 4 /m		
OP1	18.080 10	82.669 56	34.0	22.9	194			2.60	21.30			23.90	0.539
OP4	18.036 00	82.701 23	81.8	350.0	495			1.06	6.39			7.45	0.485
OP5	18.067 73	82.664 45	18.8	39.3	308			3.18	25.30			28.48	0.789
OP7	18.092 49	82.671 75	11.8	38.1	307			1.59	6.16			7.75	0.951
OP8	18.093 81	82.670 82	178.0	134.0	636			0.75	5.41			6.16	0.432
OP9	18.188 40	82.698 79	176.0	402.0	1 075			1.19	5.87			7.06	0.759
OP10	18.088 56	82.677 34	10.3	67.8				6.90				6.90	0.436
OP13	18.069 07	82.695 53	19.0	44.0				2.34				2.34	0.831
OP14	18.046 30	82.692 76	148.0	25.5	125			1.40	23.10			24.50	0.921
OP16	18.091 64	82.671 08	49.9	9.83	1 818			5.57	3.52			9.09	1.060
OP17	18.090 29	82.673 93	109.0	425.0				18.50				18.50	0.971
OP18	18.129 48	82.637 22	229.0	361.0	148			0.89	7.03			7.92	0.535
OP19	18.128 51	82.629 85	365.0	121.0	89.2	188		0.75	4.69	31.00		36.44	0.719
OP20	18.095 74	82.670 31	154.0	42.8	392			0.75	30.70			31.45	1.180
OP21	18.096 42	82.670 66	82.1	47.7	183			0.90	17.00			17.9	0.938
OP22	18.080 95	82.661 79	15.3	40.0	1 423			1.36	6.66			8.02	1.540
OP23	18.075 07	82.657 56	18.7	41.3	180			1.35	6.98			8.33	0.909
OP24	18.125 71	82.644 24	74.2	30.6	64.4			2.38	10.20			12.58	0.581
OP25	18.124 66	82.644 70	70.1	35.9	150			4.81	16.00			20.81	0.741
OP26	18.074 12	82.658 08	20.6	133.0				2.43				2.43	1.020
OP27	18.101 06	82.673 37	357.0	55.9	478			1.28	15.70			16.98	1.990
OP28	18.100 11	82.673 47	329.0	55.9	473			1.24	18.80			20.04	0.728
P1	18.089 17	82.587 22	165.0	63.79	934			5.41	13.50			18.91	1.460
P2	18.090 28	82.654 44	177.0	25.6	14 755			3.59	8.12			11.71	4.340
P3	18.090 56	82.638 89	70.4	145.3	209			3.16	23.10			26.26	0.522
P4	18.091 10	82.641 11	122.0	39.5	313			10.80	28.90			39.70	1.220
P5	18.091 10	82.639 44	91.7	49.6	4 051			10.90	25.10			36.00	0.635
P6	18.093 89	82.673 63	102.0	38.0	1 558			11.40	16.50			27.90	0.711
P7	18.099 11	82.640 00	89.2	45.3	214			1.97	5.08			7.05	0.752
P8	18.093 89	82.654 10	36.3	199.0				6.37				6.37	1.870
P9	18.096 67	82.606 94	9.76	3 000				27.40				27.40	1.220
P10	18.096 67	82.590 83	30.0	8.20	276			1.30	19.00			20.30	2.050
P11	18.093 06	82.594 72	143.0	9.00	450			1.40	10.00			11.40	1.590
P12	18.093 89	82.594 44	14.2	41.0	9.11	2 000		1.50	2.58	11.10		15.18	0.869
P13	18.068 06	82.599 70	12.7	6.55	17.7	3 201		1.54	3.87	19.50		24.91	1.600
P14	18.084 17	82.599 17	13.4	30.8	101			10.80	7.78			18.58	0.894
P15	18.080 00	82.607 22	94.7	21.3	132			1.75	18.00			19.75	1.780
P16	18.080 28	82.606 39	6.23	16.3	1 591			9.52	4.25			13.77	1.910
P17	18.078 33	82.603 89	14.5	39.4	109			9.91	21.10			31.01	0.631
P18	18.079 72	82.603 61	11.8	8 787				16.10				16.10	1.040
P19	18.068 06	82.599 72	123.0	24.5	3 000			1.20	16.20			17.40	2.240
P20	18.069 17	82.606 94	17.7	31.4	432			3.21	22.20			25.41	1.030
P21	18.068 06	82.599 72	5.63	3 000				11.50				11.50	1.900
P22	18.096 39	82.596 67	5.59	20.6	3 480			7.36	7.55			14.91	3.630

Table 4 (continued)

VES code	Latitude degrees	Longitude degrees	True resistivity					Thickness				Total thickness /m	RMS error /%
			ρ 1 /Ω·m	ρ 2 /Ω·m	ρ 3 /Ω·m	ρ 4 /Ω·m	ρ 5 /Ω·m	h 1 /m	h 2 /m	h 3 /m	h 4 /m		
P23	18.070 56	82.671 39	19.2	8.33	581			1.69	23.50			25.19	1.440
P24	18.071 11	82.671 94	18.8	8.25	2 390			1.81	30.90			32.71	1.450
P25	18.093 61	82.686 92	68.7	14.2	761			1.50	10.50			12.00	1.430
P26	18.093 33	82.688 89	82.0	15.4	17.2	19.2	885	1.56	1.79	3.06	10.80	17.21	0.616
P27	18.096 67	82.686 11	5.58	13.0	593			3.61	40.00			43.61	0.545
P28	18.097 78	82.685 56	6.87	14.7	6.8	1 284		3.28	2.01	21.20		26.49	1.460
P29	18.098 06	82.685 83	6.74	13.0	1 284			5.93	29.80			35.73	1.000
P30	18.097 78	82.686 39	6.36	10.3	3 232			6.97	30.70			37.67	1.070
P31	18.100 56	82.690 83	5.19	37.2	131			5.18	29.10			34.28	0.532
P32	18.099 72	82.691 11	5.02	84.8				5.60				5.60	2.220
P33	18.076 12	82.678 21	9.31	12.0	652			1.78	59.40			61.18	2.160
P34	18.081 82	82.684 10	6.26	27.2	7.09	3 161		2.80	4.27	17.20		24.27	2.020
P35	18.076 11	82.678 06	6.18	62.9				17.50				17.50	1.560
P36	18.078 61	82.676 94	5.89	60.0				12.50				12.50	1.450
P37	18.077 22	82.678 61	5.36	18.3	890			15.20	2.66			17.86	2.620
P38	18.077 22	82.678 22	5.34	25.6	890			14.70	59.20			73.90	2.440
P39	18.090 56	82.667 50	178.0	43.3	13 105			2.14	22.00			24.14	3.000
P40	18.090 28	82.666 70	44.9	21.9	161			1.50	8.55			10.05	1.870
P41	18.109 44	82.680 10	7.14	124.0				11.80				11.80	1.440
P42	18.110 83	82.680 18	6.91	129.0				10.70				10.70	2.200
P43	18.104 72	82.646 67	190.0	19.5	6 000			1.20	18.00			19.20	2.190
P44	18.105 00	82.647 78	93.6	34.3	203			1.50	5.39			6.89	2.230
P45	18.104 72	82.612 20	152.0	13.8	1 278			1.00	6.70			7.70	2.120
P46	18.105 00	82.652 22	54.4	82.8	9 659			4.13	32.90			37.03	0.721
P47	18.141 11	82.690 00	59.4	103.0	714			3.10	26.20			29.30	0.617
P48	18.144 40	82.690 00	87.5	31.0	97.3			1.50	8.57			10.07	0.350
P49	18.141 11	82.690 00	107.0	46.6	96.5	665		1.50	2.55	22.20		26.25	1.110
P50	18.095 28	82.672 20	94.7	50.0	3 144			1.92	29.10			31.02	1.360

isotropic in nature. If they are not equal then the layers are considered to be anisotropic.

2.3.3 Longitudinal resistivity and Transverse resistivity

The longitudinal resistivity (ρ_l) and transverse resistivities (ρ_t) can be calculated as

$$\rho_l = \frac{H}{S} \tag{3}$$

$$\rho_t = \frac{T}{H} \tag{4}$$

Where: H is the thickness of all layers, S is the total longitudinal conductance, and T is the total transverse resistance.

2.3.4 Coefficient of Anisotropy

The coefficient of anisotropy (λ) measures the anisotropic extent of an aquifer system (Singh et al. 2021). It can be calculated as:

$$\lambda = \sqrt{\rho_t / \rho_l} \tag{5}$$

Where: ρ_t refers to the transverse resistivity, and the ρ_l represents the longitudinal resistivity. The areas with higher values of λ are associated with low porosity and permeability (Gupta et al. 2015). In most geological conditions, the electrical anisotropy is 1 and does not exceed 2 (Anudu et al. 2011). Singh and Singh (1970) pointed out that lower values of λ correspond to high aquifer potential zones. The spatial distribution maps (Fig.5a, Fig.5b, Fig.5c, Fig.5d, and Fig.5e) have been prepared for these Dar zarrouk parameters.

2.4 Aquifer parameters

Hydraulic conductivity (K) is a crucial hydrogeo-

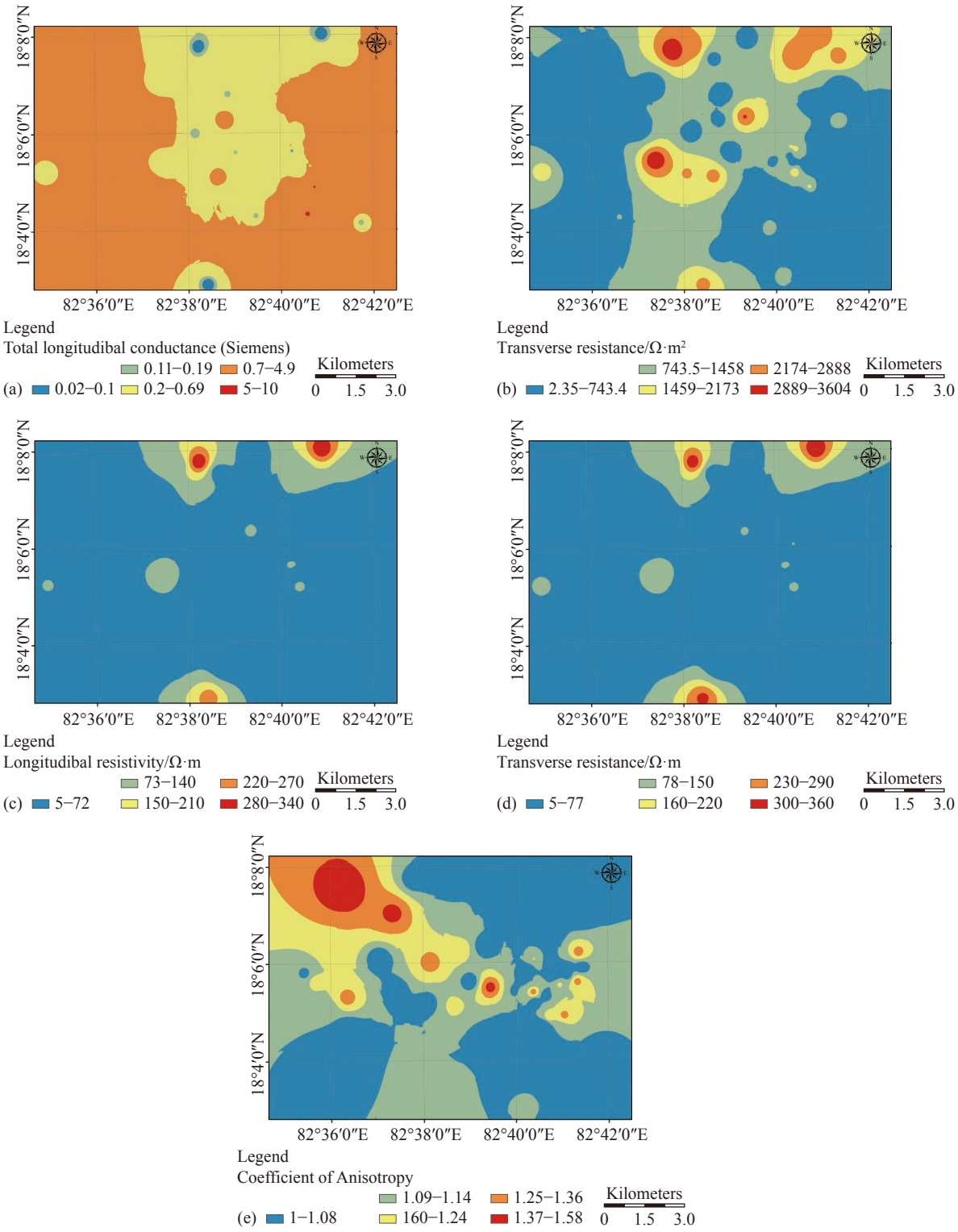

Fig. 5 Spatial distribution maps of (a) Total longitudinal conductance (b) Total transverse resistance (c) Longitudinal resistivity (d) Transverse resistivity (e) Coefficient of anisotropy of the study area

logical parameter that controls the movement of fluids and contaminants through the subsurface, particularly in solid and and porous aquifers, along with other parameters (Elango, 2014). Transmissivity is another parameter that helps us understand the groundwater potential, secondary porosity, and hydrogeological conditions of a groundwater development area (Kumar et al. 2016). The aquifer' s hydraulic conductivity (K) and aquifer transmissivity (T_r) can be determined from D-Z parameters. The hydraulic conductivity of an aquifer is defined as its ability to transport

water under the influence of a hydraulic gradient, while the transmissivity refers to the aquifer' s ability to transmit groundwater throughout its entire saturated thickness (Todd, 1980). Areas with high transmissivity values are usually indicative of high water-bearing potential (Obiora et al. 2016). According to Todd' s (1980) equation, the relationship between the aquifer transmissivity (T_r) and hydraulic conductivity (K) can be expressed as follows:

$$K = 386.40R_{rw}^{-0.932\,83} \quad (6)$$

Where: R_{rw} is the aquifer resistivity (i.e. resistivity of the inferred aquiferous layer from the interpreted curves). The hydraulic conductivity (K) can be determined from the formula (Equation 6) given by Heigold et al. (1979)

$$T_r = K\sigma T \quad (7)$$

Where: σ is electrical conductivity and T is transverse resistance.

3 Results and discussions

3.1 Primary geo-electrical parameters (True resistivity/thickness of layers)

The interpreted VES results indicate that the true resistivity of the first layer ranges from 5.02 Ω·m to 365 Ω·m, with an average of 72.86 Ω·m, and its thickness ranges from 0.75 m to 27.4 m (average: 5.07 m). The second layer' s true resistivity varies from 6.55 Ω·m to 8 787 Ω·m (average: 267.92 Ω·m), and its thickness varies from 1.79 m to 59.4 m (average: 16.40 m). The third layer' s true resistivity ranges from 6.8 Ω·m to 14 755 Ω·m (average: 1 460.14 Ω·m), and its thickness ranges from 3.06 m to 31 m (average: 17.89 m). The fourth layer's true resistivity ranges from 19.2 Ω·m to 3 201 Ω·m (average: 1 502.60 Ω·m) and it has a thickness of 10.8 m (Table 4).

The results indicate that the true resistivity some layers at certain locations is less than 10 Ω·m, which may be attributed to highly weathered, sandy clay or highly saturated formation. Based on the classification of Venkateswara et al. (2019b) for inferred lithology in the Eastern Ghats mobile belt of Andhra Pradesh using VES results, the subsurface lithology in the present study area can be inferred as shown in Table 5.

The aquifer resistivity in the hard rocks of the Eastern Ghats falls within the range of 10 Ω·m to 150 Ω·m (Venkateswara et al. 2019b). However, aquifer formations with resistivities less than 10 Ω·m are also observed, which can be attributed to highly weathered or saturated formations. Therefore, for the present study area, the aquifer resistivity range between 5 Ω·m and 150 Ω·m has been considered. The aquifer thickness in the study area ranges from 1.1 m to 74 m, with the maximum thickness (74 m) observed in the eastern part (Fig. 4a). However, most of the study area has an aquifer thickness of 12 m to 32 m, except for a few patches in the east, southeast, central, south, and north. On average, the aquifer thickness is greater than 33 m in the eastern, central, and south-eastern parts of the study area (Fig. 4a). In the eastern side of the study area, a long and NNE-SSW directed lineament has been identified, which is surrounded by a 25 km^2 area of the pediment-pediplain complex zone. The sediments eroded from the dissected hills are deposited in this zone which may explain high thickness observed in this area.

The basement depth in the study area ranges from 2.4 m to 74 m (Fig. 4b). The spatial distribution map of basement depth indicates that most of the area falls within the range of 14 m to 33 m, except for a few areas on the eastern, central, and northern sides that exceed the 33-meter depth. In the eastern region, two small patches on the east side show a deeper basement depth ranging from 65 m to 74 m (Fig. 4b). The higher values of basement depth in these areas are attributed to rock weathering, which is more pronounced in the central to eastern parts of the study area.

3.2 Secondary geo-electrical parameters (D-Z parameters)

Longitudinal conductivity (S) is defined as the ability of current to flow through the sub-surface layers and has direct relationship with both hydraulic conductivity (K) and aquifer transmissivity (T_r), which are parameters of aquifer flow.

Table 5 Resistivity range of subsurface layers (After Venkateswara et al. 2019b)

No	Resistivity (Ω·m)	Formation
1	<10	Clayey sand/highly weathered/highly saturated formation
2	10–60	Weathered formations
3	61–150	Semi-weathered/fractured formation
4	>150	Hard rock

Transverse resistance (T) reflects the highly permeable (less porous) nature of the formation, with transmissivity and transverse resistance showing a meaningful relationship due to the direct linear relationship between hydraulic conductivity and resistivity, as per Darcy and Ohm's law (Sri and Singhal, 1981).

The total longitudinal conductance (S) values in the present study area vary from 0.02 Siemens to 5.1 Siemens (Table 6), with the spatial distribution map of S (Fig. 5a) showing that most of the study area has S values ranging between 0.2 Siemens and 4.9 Siemens, and indicating that the study area has moderate to good aquifer protective capacity. The higher values of S are observed on the eastern and western sides of the study area, attributed to the highly porous material along the streams and sediments deposited in pediment-pediplain complex zones on both sides (E&W) of the study area.

The T values in the study area range from 28.35 $\Omega\cdot m^2$ to 3 604 $\Omega\cdot m^2$ (Table 6), with the spatial distribution map of T (Fig. 5b) clearly showing that higher values (>743.5 $\Omega\cdot m^2$) occur in the north-south direction and at the NNE corner. The lower values (<743.5 $\Omega\cdot m^2$) on the east and west sides of the study area, is possibly due to the presence of highly porous material in the pediment-pediplain complex zone on the eastern side, discontinued patches of pediment-pediplains on the western side, and structural lineaments. The higher values of T are observed in the N-S and NE parts of the study area, attributed to the poorly weathered and fractured rocks at these locations.

In the study area, the longitudinal resistivity (ρ_l)

Table 6 Secondary geoelectrical parameters and transmissivity values

VES code	Latitude degrees	Longitude degrees	Longitudinal conductance (S)/siemens	Transverser esistance (T)/Ωm^2	Anisotropy (λ)	Longitudinal resistivity (ρ_l)/Ω·m	Transverse resistivity (ρ_t)/Ω·m	Aquifer transmissivity (T_r)/m^2/d
OP1	18.080 10	82.669 56	1.01	576.17	1.01	23.74	24.11	523.91
OP4	18.036 00	82.701 23	0.03	2 323.21	1.14	238.66	311.84	180.34
OP5	18.067 73	82.664 45	0.81	1 054.07	1.03	35.03	37.01	337.46
OP7	18.092 49	82.671 75	0.30	253.46	1.12	26.14	32.70	86.16
OP8	18.093 81	82.670 82	0.04	858.44	1.00	138.16	139.36	35.50
OP9	18.188 40	82.698 79	0.02	2 569.18	1.05	330.47	363.91	45.36
OP10	18.088 56	82.677 34	0.67	71.07	1.00	10.30	10.30	302.75
OP13	18.069 07	82.695 53	0.12	44.46	1.00	19.00	19.00	58.00
OP14	18.046 30	82.692 76	0.92	796.25	1.10	26.77	32.50	588.14
OP16	18.091 64	82.671 08	0.47	312.54	1.33	19.35	34.38	63.07
OP17	18.090 29	82.673 93	0.17	2 016.50	1.00	109.00	109.00	89.87
OP18	18.129 48	82.637 22	0.02	2 741.64	1.01	339.04	346.17	67.66
OP19	18.128 51	82.629 85	0.39	3 606.44	1.03	93.83	98.97	236.81
OP20	18.095 74	82.670 31	0.72	1 429.46	1.02	43.55	45.45	388.07
OP21	18.096 42	82.670 66	0.37	884.79	1.01	48.73	49.43	194.80
OP22	18.080 95	82.661 79	0.26	287.21	1.07	31.40	35.81	88.86
OP23	18.075 07	82.657 56	0.24	313.52	1.04	34.54	37.64	91.19
OP24	18.125 71	82.644 24	0.37	488.72	1.06	34.43	38.85	253.77
OP25	18.124 66	82.644 70	0.51	911.58	1.04	40.46	43.80	347.62
OP26	18.074 12	82.658 08	0.12	50.06	1.00	20.60	20.60	55.85
OP27	18.101 06	82.673 37	0.28	1 334.59	1.15	59.70	78.60	216.24
OP28	18.100 11	82.673 47	0.34	1 458.88	1.11	58.93	72.80	236.38
P1	18.089 17	82.587 22	0.24	1 753.82	1.09	77.37	92.75	220.16
P2	18.090 28	82.654 44	0.34	843.30	1.44	34.70	72.02	618.20
P3	18.090 56	82.638 89	0.20	3 578.89	1.03	128.81	136.29	91.52
P4	18.091 10	82.641 11	0.82	2 459.15	1.13	48.40	61.94	779.60
P5	18.091 10	82.639 44	0.62	2 244.49	1.04	57.61	62.35	458.22
P6	18.093 89	82.673 63	0.55	1 789.80	1.12	51.10	64.15	611.49

Table 6 (continued)

VES code	Latitude degrees	Longitude degrees	Longitudinal conductance (S)/siemens	Transverser esistance (T)/Ωm^2	Anisotropy (λ)	Longitudinal resistivity (ρ_l)/Ω·m	Transverse resistivity (ρ_t)/Ω·m	Aquifer transmissivity (T_r)/m^2/d
P7	18.099 11	82.640 00	0.13	405.85	1.05	52.52	57.57	98.73
P8	18.093 89	82.654 10	0.18	231.23	1.00	36.30	36.30	86.31
P9	18.096 67	82.606 94	2.81	267.42	1.00	9.76	9.76	1 264.15
P10	18.096 67	82.590 83	2.36	194.80	1.06	8.60	9.60	1 289.37
P11	18.093 06	82.594 72	1.12	290.20	1.58	10.17	25.46	1 604.52
P12	18.093 89	82.594 44	1.39	228.20	1.17	10.94	15.03	1 232.45
P13	18.068 06	82.599 70	1.81	390.06	1.07	13.73	15.66	583.50
P14	18.084 17	82.599 17	1.06	384.34	1.09	17.55	20.69	197.08
P15	18.080 00	82.607 22	0.86	549.13	1.10	22.87	27.80	574.35
P16	18.080 28	82.606 39	1.79	128.58	1.10	7.70	9.34	225.57
P17	18.078 33	82.603 89	1.22	975.04	1.11	25.44	31.44	310.62
P18	18.079 72	82.603 61	1.36	189.98	1.00	11.80	11.80	622.27
P19	18.068 06	82.599 72	0.67	544.50	1.10	25.93	31.29	434.52
P20	18.069 17	82.606 94	0.89	753.90	1.02	28.60	29.67	372.42
P21	18.068 06	82.599 72	2.04	64.75	1.00	5.63	5.63	886.42
P22	18.096 39	82.596 67	1.68	196.67	1.22	8.86	13.19	219.43
P23	18.070 56	82.671 39	2.91	228.20	1.02	8.66	9.06	1 465.24
P24	18.071 11	82.671 94	3.84	288.95	1.02	8.51	8.83	1 890.23
P25	18.093 61	82.686 92	0.76	252.15	1.15	15.76	21.01	577.46
P26	18.093 33	82.688 89	0.73	674.97	1.29	23.65	39.22	862.81
P27	18.096 67	82.686 11	3.72	540.14	1.03	11.71	12.39	1 467.18
P28	18.097 78	82.685 56	3.73	196.24	1.02	7.10	7.41	1 865.21
P29	18.098 06	82.685 83	3.17	427.37	1.03	11.26	11.96	1 160.85
P30	18.097 78	82.686 39	4.08	360.54	1.02	9.24	9.57	1 535.85
P31	18.100 56	82.690 83	1.78	1 109.40	1.30	19.25	32.36	394.94
P32	18.099 72	82.691 11	1.12	28.11	1.00	5.02	5.02	480.38
P33	18.076 12	82.678 21	5.14	729.37	1.00	11.90	11.92	2 312.66
P34	18.081 82	82.684 10	3.03	255.62	1.15	8.01	10.53	2 241.18
P35	18.076 11	82.678 06	2.83	108.15	1.00	6.18	6.18	1 236.57
P36	18.078 61	82.676 94	2.12	73.63	1.00	5.89	5.89	923.76
P37	18.077 22	82.678 61	2.98	130.15	1.10	5.99	7.29	1 959.43
P38	18.077 22	82.678 22	5.07	1 594.02	1.22	14.59	21.57	1 168.54
P39	18.090 56	82.667 50	0.52	1 333.52	1.09	46.41	55.24	353.98
P40	18.090 28	82.666 70	0.42	254.60	1.03	23.71	25.33	252.37
P41	18.109 44	82.680 10	1.65	84.25	1.00	7.14	7.14	728.73
P42	18.110 83	82.680 18	1.55	73.94	1.00	6.91	6.91	681.29
P43	18.104 72	82.646 67	0.93	579.00	1.21	20.66	30.16	718.29
P44	18.105 00	82.647 78	0.17	325.28	1.09	39.79	47.21	135.47
P45	18.104 72	82.612 20	0.49	244.46	1.42	15.65	31.75	591.63
P46	18.105 00	82.652 22	0.47	2 948.79	1.01	78.24	79.63	223.59
P47	18.141 11	82.690 00	0.31	2 882.74	1.01	95.58	98.39	143.34
P48	18.144 40	82.690 00	0.29	396.92	1.07	34.30	39.42	201.00
P49	18.141 11	82.690 00	0.30	2 421.63	1.02	87.85	92.25	136.58
P50	18.095 28	82.672 20	0.60	1 636.82	1.01	51.50	52.77	329.02

ranges from 5 Ω·m to 340 Ω·m. Except for a few locations, most of the study area has lower ρl between 5 Ω·m and 72 Ω·m. Higher values of ρl (>73 Ω·m) are observed in the south, north, and northeast regions (Fig. 5c). The transverse resistivity ρt ranges from 5 Ω·m to 360 Ω·m, with lower values (5 Ω·m to 77 Ω·m) observed for most of the study area, and higher values (>78 Ω·m) observed in the south, north, and northeast regions (Fig. 5d). These values suggest an inhomogeneous and anisotropic subsurface lithology.

The coefficient of anisotropy (λ) in the study area varies from 1 to 1.58, with most of the area exhibiting lower values (1 to 1.14) and higher values (>1.37) observed in the northwest and central regions, as indicated by the spatial distribution map of λ (Fig. 5e). The lower values of electrical anisotropy suggest the presence of good to moderated potentiality of aquifers and deeper basement depth in the study area.

3.3 Hydro-geological parameters

The aquifer transmissivity (T_r) values in the present study area range from 35.5 m^2/d to 2 312 m^2/d (Table 6). A spatial distribution map of the aquifer transmissivity (T_r) has been generated and shown in Fig. 6.

The lower values of T_r have been mostly observed in the central part of the area, while higher T_r values were found in the east, southeast, and northwestern corners. A long linear zone with high transmissivities is observed along the NNE-SSW direction towards the eastern side. Additionally, a 9.6 km lineament has been identified along this zone (Fig. 2).

Based on the aquifer transmissivity values, all locations are classified according to the groundwater potential classification provided by Offodile (1983) and Venkateswara et al. (2022) into categories of good, moderate, low, very low, and negligible groundwater potential (Table 7 and Fig. 7). Out of the 72 groundwater locations, 31 were classified as having good potential, 39 as having moderate potential, and 2 as having low potential. To better understand the geomorphology of the study area, the classified potential groundwater locations and lineaments were superimposed on a recent (16th March 2022) Landsat-8 Satellite image.

After analyzing the aquifer transmissivity values and aquifer thickness in the study area, it was observed that out of the 31 locations classified as having good potential groundwater (T_r > 500 m^2/d), only the 16 of them (OP1, OP14, P4, P6, P9, P10, P13, P23, P24, P27, P28, P29, P30, P33, P34, and P38) have aquifer thicknesses greater than 20 m and transmissivity values greater than 500 m^2/d. Although the remaining good potential groundwater locations have T_r values greater than 500 m^2/d, they have less than 20 m thickness of aquifers. Only 6 of the 16 good potential ground-

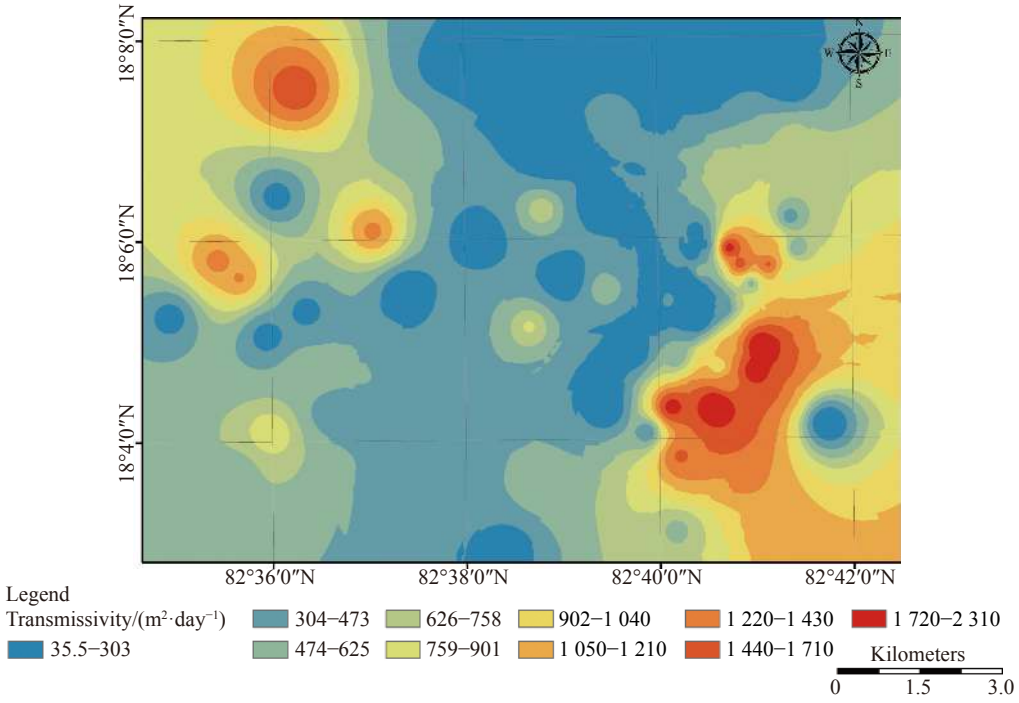

Fig. 6 Spatial distribution map of aquifer transmissivity (T_r) of the study area

Table 7 Aquifer classification based on the transmissivity values (Offodile, 1983; Venkateswara et al. 2022)

Transmissivity (T_r) /m^2/d	Classification of aquifers	No of sounding points based on T_r value
>500	Good potential	31
50–500	Moderate potential	39
5–50	Low potential	02
0.5–5	Very low potential	-
<0.5	Negligible potential	-

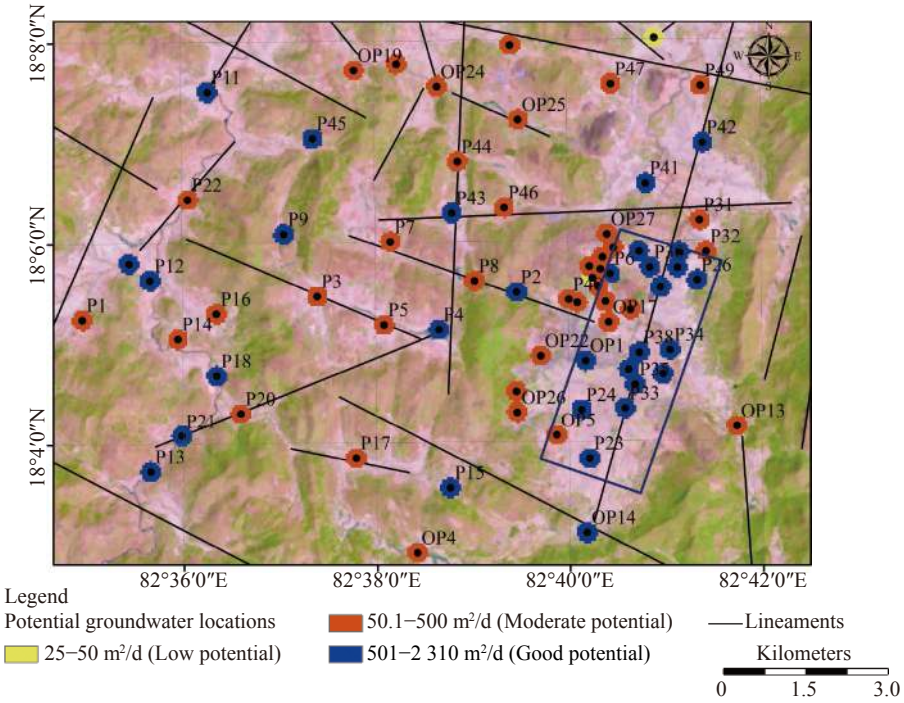

Fig. 7 Map of potential groundwater locations based on aquifer transmissivity values

water locations (P24, P27, P29, P30, P33, and P38) have an aquifer thickness greater than 30 m, which makes them suitable for yielding a significant quantity of groundwater. The remote sensing analysis revealed that a long (9.6 km) lineament on the eastern side of the study area, oriented in the NNE-SSW direction, is located in a pediment-pediplain complex zone, characterized by a good (>30 m) thickness of the aquifer and deeper basement depth. The analysis of D-Z parameters shows that this portion of the study area exhibits high longitudinal conductivity (0.7–4.9 Siemens) and low electrical anisotropy (λ) (1–1.14), which are highly favorable for groundwater occurrence. Based on these characteristics, drilling recommendations may be made for these six good potential groundwater locations.

The analysis also revealed that out of the 39 locations classified as having moderate potential groundwater (T_r: 50–500 m^2/d, only 15 of them (OP5, OP14, OP19, OP20, OP25, P3, P5, P17, P20, P31, P39, P46, P47, P49, and P50) have aquifer thickness greater than 20 m. However, out of these 15 locations, only 3 (OP19, P5, and P46) have high (>30 m) aquifer thickness. These three locations are located along the N-S direction in the central region. The analysis of D-Z parameters also revealed that the low longitudinal conductance (0.02 Siemens to 2.1 Siemens) at these locations indicates that the aquifer is of moderate to good protective capacity. The anisotropy coefficient also shows lower values (1 to 1.14) at all these three locations, which is a good indicator of a deep basement. Although the remaining moderately potential groundwater locations have aquifer T_r values of 50–500 m^2/d, they only have an aquifer thickness of less than 20 m.

4 Conclusion

Based on the analysis of the Dar-Zarrouk and aquifer parameters, a linear groundwater potential zone (8.46 km^2) in the eastern part of the study area, extending in NNE-SSW direction along a

long lineament of 9.6 km, was identified. Of the 16 VES locations classified as good groundwater potential based on aquifer transmissivity values, six locations (P24, P27, P29, P30, P33, and P38) exhibit good aquifer thickness (> 30 m) and are recommended as excellent sources for groundwater exploration. The remaining 10 locations in this zone exhibit moderate thickness (20–30 m). Aquifer thickness in this zone is obtained from sediments derived from the weathering and transportation of existing dissected hills. Total longitudinal conductance values in this zone (0.7–4.9 Siemens) reveal that the aquifer is under good protective capacity. Additionally, three locations (OP19, P5, and P46) in the central region, exhibiting high aquifer thickness (> 30 m) from the weathering of rocks are recommended for drilling bore wells. Other locations (OP14, OP20, P4, P10, P12, P13, P15, P17, P18, P31, P46, and P50) along streams in the western and central part of the area exhibit moderate aquifer thickness (20–30 m) and can yield reasonable quantities of water. This information is beneficial for groundwater exploration and watershed management to meet the demand of the tribal people in the area.

Acknowledgement

We sincere thanks to the anonymous reviewers and specially to the editor for critically reviewing our paper that helped us to improve its quality. We also express our gratitude to the language experts for their help in arranging the script as per journal guidelines.

References

Ammar AI, Kruse SE. 2016. Resistivity soundings and VLF profiles for siting groundwater wells in a fractured basement aquifer in the Arabian shield, Saudi Arabia. Journal of African Earth Sciences, 116: 5667. DOI：10.1016/j.jafrearsci.2015.12.020.

Anandagajapathi RB, Venkateswara RP, Subrahmanyam M. 2020. Integration of GIS and remote sensing in groundwater investigations: A case study from Visakhapatnam District, India. Journal of India Geophysics Union, 24(5): 50−63.

Ankidawa B, Ishaku J, Hassan A. 2019. Estimation of aquifer transmissivity using Dar-Zarrouk parameters derived from resistivity soundings on the floodplain of river Dadin kowa, Gombe state, Northeastern Nigeria. Computer Engineering Physics Model, 1(4): 36−52. DOI：10.22115/cepm.2018.129584.1024.

Anudu GK, Onuba LN, Ufondu LS. 2011. Geoelectric sounding for groundwater exploration in the crystalline basement terrain around onipe and adjoining areas, Southwestern Nigeria. Journal of Applied Technology in Environmental Sanitation, 1: 343−354.

Atakpo EA. 2013. Aquifer vulnerability investigation using geo-electric method in parts of sapele local government area of delta state, Nigeria. Nigerian Journal of Basic Application Science, 21(1): 11−19. DOI：10.4314/njbas.v21i1.2.

Awni T, Batayneh. 2013. The estimation and significance of Dar-Zarrouk parameters in the exploration of quality affecting the Gulf of Aqaba coastal aquifer systems. Journal of Coast Conservation, 17: 623−635. DOI：10.1007/S11852-013-02614.

Ayolabi EA, Folorunso AF, Oloruntola MO. 2010. Constraining causes of structural failure using electrical resistivity tomography (ERT): A case study of Lagos, Southwestern, Nigeria. Mineral Wealth, 156(4): 7−18. DOI：10.3997/2214-4609-pdb.175.SAGEEP109.

Bobachev A. 2003. Resistivity sounding interpretation IPI2WIN: Version 3.0. 1, A7. 01. 03. Moscow State University.

CGWB. 2019. Groundwater brochure Visakhapatnam district, Andhra Pradesh, central ground water board, Ministry of water resources, government of India.

Danso SY, Ma Y. 2023. Geospatial techniques for groundwater potential zones delineation in a coastal municipality, Ghana. The Egyptian Journal of Remote Sensing and Space Science, 26(1): 75−84. DOI：https://doi.org/10.1016/j.ejrs.2022.12.004.

Deng QJ, Wei LI, Zhu QJ, et al. 2020. An analysis of the characteristics of water storage structure and the practice of groundwater exploration in the basalt area of Zhangbei County, Bashang, Hebei Province. Geological Bulletin of China, 39(12): 1899−1907.

Dor N, Syafalni S, Abustan I, et al. 2011. Verification of surface-groundwater connectivity in an irrigation canal using geophysical, water balance and stable isotope approaches. Water Resource Manage, 25: 2837–2853. https://doi.org/10.1007/s11269-011-9841-y

Elango L. 2014. Hydraulic conductivity issues, determinations and application. Croatia Envir-

onmental Processes, 1: 613−616. DOI：10.1007/s40710-000337.

Fashae OA, Tijani MN, Talabi AO, et al. 2014. Delineation of groundwater potential zones in the crystalline basement terrain of SW-Nigeria: An integrated GIS and remote sensing approach. Journal of Applied Water Science, 4: 19–38. https://doi.org/10.1007/s13201-013-0127-9

GSI. 2001. District resource map, geological survey of India. Visakhapatnam district, Andhra Pradesh, India.

Gumilar UN, Andi AN, Pulung AP, et al. 2023. Analysis of groundwater potential zones using Dar-Zarrouk parameters in Pangkalpinang city, Indonesia. Environment, Development and Sustainability, 25: 1876−1898. DOI：10.1007/s10668-021-02103-7.

Gupta G, Patil SN, Padmane ST, et al. 2015. Geoelectric investigation to delineate groundwater potential and recharge zones in Suki river basin, north Maharashtra. Journal of Earth System Science, 124(7): 1487−1501. DOI：10.1007/s12040-015-0615-4.

Gupta G, Vinit CE, Saumen M. 2012. Geo-electrical investigation for potential groundwater zones in parts of Ratnagiri and Kolhapur districts, Maharashtra. Journal of India Geophysics Union, 9(1): 27−38.

Hamzah U, Samudin AR, Malim EP. 2007. Groundwater investigation in Kuala Selang or using vertical electric sounding (VES) surveys. Environmental Geology, 51: 1349–1359. https://doi.org/10.1007/s00254-006-0433-8

Heigold PC, Gilkeson RH, Cartwright K, et al. 1979. Aquifer transmissivity from surficial electrical methods. Ground Water, 17(4): 338−345. DOI：10.1111/J.1745-6584.1979.Tb03326.X.

Kang X, Shi X, Deng Y, et al. 2018. Coupled hydro-geophysical inversion of DNAPL source zone architecture and permeability field in a 3D heterogeneous sandbox by assimilation time-lapse cross-borehole electrical resistivity data via ensemble kalman filtering. Journal of Hydrology, 567: 149−164. DOI：10.1016/J.JhydrOl.2018.10.019.

Kumar TJR, Balasubramanian A, Kumar RS, et al. 2016. Assessment of groundwater potential based on aquifer properties of hard rock terrain in the Chittar–Uppodai watershed, Tamil Nadu, India. Applied Water Science, 6: 179−186. DOI：10.1007/s13201-014-0216-4.

Loke MH, Chambers JE, Rucker DF, et al. 2013. Recent developments in the direct-current geoelectrical imaging method. Journal of Applied Geophysics, 95: 135−156. DOI：10.1016/J.Japp.geo.2013.02.017.

Maillet R. 1947. The fundamental equations of electrical prospecting. Geophysics, 12(4): 529−556. DOI：10.1190/1.1437342.

Maja B, Andrej S, Ivan KC, et al. 2020. Characterization of aquifers in metamorphic rocks by combined use of electrical resistivity tomography and monitoring of spring hydrodynamics. Geosciences, 10: 137. DOI：10.3390/Geosciences10040137.

Obiora DN, Ibuot JC, George JN. 2016. Evaluation of aquifer potential, geo-electric and hydraulic parameters in Ezza north, southeastern Nigeria, using geo-electric sounding. International Journal of Environmental Science and Technology, 13: 435−444. DOI：10.1007/S13762-015-0886-Y.

Offodile MI. 1983. The occurrence and exploitation of groundwater in Nigeria basement complex. Journal of Mining Geology, 20(3): 131−146.

Oladapo MI, Akintorinwa OJ. 2007. Hydrogeophysical study of Ogbese southwestern Nigeria. Global Journal of Pure Applied Science, 13(1): 55–61. https://doi.org/10.4314/gjpas.v13i1.16669

Olasehinde, PI, Bayewu OO. 2011. Evaluation of electrical resistivity anisotropy in Geological mapping: A case study of Odo area, west central Nigeria. African Journal of Environmental Science and Technology, 5(7): 553−566. DOI：10.4314/ajest.v5i7.72045.

Orellana E, Mooney HM. 1966. Master curves for Schlumberger arrangement. Madrid, P. 34.

Oteri AU. 1981. Geo-electric investigation of saline contamination of chalk aquifer by mine drainage water at Tilmanstone, England. Geoexploration, 19(3): 179–192. https://doi.org/10.1016/0016-7142(81)90002-8

Rustadi, Darmawan IGB, Haerudin N, et al. 2022. Groundwater exploration using integrated geophysics method in hard rock terrains in Mount Betung Western Bandar Lampung, Indonesia. Journal of Groundwater Science and Engineering, 10(1): 10−18. DOI：10.19637/j.cnki.2305-7068.2022.01.002.

Sathiyamoorthy M, Madhavi G. 2018. Delineation of groundwater potential and recharge zone using electrical resistivity method around Veeranam Tank, Tamil Nadu, India. Journal of the Institution of Engineers (India), Series

A 99.4 (2018): 637−645. https://doi.org/10.1007/s40030-018-0318-3

Seker UE, Efe S. 2023. Comparative economic analysis of air conditioning system with groundwater source heat pump in general-purpose buildings: A case study for kayseri. Renewable Energy, 204: 372−381.

Shailaja G, Gupta G, Suneetha N, et al. 2019. Assessment of aquifer zones and its protection via second-order geo-electric indices in parts of drought-prone region of deccan volcanic province, Maharashtra, India. Journal of Earth System Science, 128: 78. https://doi.org/10.1007/s12040-019-1104-y

Singh S, Gautam PK, Kumar P, et al. 2021. Delineating the characteristics of saline water intrusion in the coastal aquifers of Tamil Nadu, India by analyzing the Dar-Zarrouk parameters. Contributions to Geophysics and Geodesy, 51(2): 141−163. https://doi.org/10.31577/congeo.2021.51.2.3

Singh CL, Singh SN. 1970. Some geo-electrical investigations for potential groundwater in part of Azamgrah area of UP. Pure and Applied Geophysics, 82: 270–85. https://doi.org/10.1007/BF00876184

Sitharam TG, Anbazhagan P, Ganesha Raj K. 2006. Use of remote sensing and seismotectonic parameters for seismic hazard analysis of Bangalore. Natural Hazards and Earth System Science, 6: 927–939. https://doi.org/10.5194/nhess-6-927-2006

Sitharam TG, Anbazhagan P. 2007. Seismic hazard analysis for the Bangalore region. Natural Hazards, 40: 261−278.

Sri N, Singhal DC. 1981. Estimation of aquifer transmissivity from Dar-Zarrouk parameters in porous media. Journal of Hydrology, 50: 393−399. DOI：10.1016/0022-1694(81)90082-2.

Subramanian TS, Marykutty A. 2019. Computation of aquifer parameters using geo-electrical techniques for the north Chennai coastal aquifer. Indian Journal of Geo Marine Sciences, 48: 1298−1306. https://doi.org/10.1007/s10668-021-02103-7

Subrahmanyam M, Venkateswara Rao P. 2017a. A note on the advantages of converting schlumberger VES data into radial dipole VES data. Journal of Geophysics, 28(4): 248−257.

Subrahmanyam M, Venkateswara RP. 2017b. Delineation of groundwater potential zones using geo-electrical surveys in SSW part of Yeleru river basin, East Godavari District, Andhra Pradesh. Journal of Indian Geophysics Union, 21(6): 465−473.

Suneetha NG, Gupta G, Shailaja G, et al. 2021. Spatial behavior of the Dar-Zarrouk parameters for exploration and differentiation of water bodies aquifers in parts of konkan coast of Maharashtra, India. Journal of Coastal Conservation, 25: 11. DOI：10.1007/S11852-021-00807-6.

Todd KD. 1980. Groundwater Hydrology, Third Ed. New York, John Wiley and Sons: 636.

Venkateswara RP, Subrahmanyam M, Ratnakar D. 2019a. Performance evaluation of different interpretation techniques of vertical electrical sounding data. Journal of Indian Geophysics Union, 23(1): 55−68.

Venkateswara RP, Subrahmanyam M, Ramdas P. 2019b. Delineation of groundwater potential zones in hard rock basement terrains of East-Godavari District, Andhra Pradesh, India. Journal of Indian Geophysics Union, 23(5): 408−419.

Venkateswara RP, Mangalampalli S, Bakuru AR. 2021. Groundwater exploration in hard rock terrains of East Godavari District, Andhra Pradesh, India using AHP and WIO analyses together with geoelectrical surveys. AIMS Geosciences, 7(2): 243−266. DOI：10.3934/geosci.2021015.

Venkateswara RP, Mangalampalli S, Bakuru AR. 2022. Investigation of groundwater potential zones in hard rock terrains along EGMB, India, using remote sensing, geoelectrical and hydrological parameters. Acta Geophysica, https://doi.org/10.1007/s11600-022-00916-2

Zohdy AAR. 1965. The auxiliary point method of electrical sounding interpretation and its relationship to the Dar-Zarrouk parameters. Geophysics, 30: 644−660. DOI：10.1190/1.1439636.

Zohdy AAR, Eaton GP, Mabey DR. 1974. Application of surface geophysics to groundwater investigations, US Geology Survey. Technology Water Resource Investigation: 116. https://doi.org/10.3133/twri02D1

Zohdy AAR. 1989. A new method for the automatic interpretation of Schlumberger and Wenner sounding curves. Geophysics, 54: 245−253. DOI：10.1190/1.1442648.